



A process of low-lying magnetic reconnection observed by THEMIS, BBSO and TRACE

L. Contarino¹, P. Romano¹, F. Zuccarello¹, and V.B. Yurchyshyn²,

¹ Dipartimento di Fisica e Astronomia, Sezione Astrofisica, Università di Catania,
Via S.Sofia 78, 95125 Catania, Italy; e-mail: lcont@ct.astro.it

² Big Bear Observatory, 40386 NorthShore Lane Big Bear City, CA 92314 - 9672
- U.S.A.

Abstract. We describe the results obtained from the study of a filament eruption associated to a two-ribbon flare, occurred in NOAA AR 9445 on May 5, 2001. We interpret the event in a two-step reconnection scenario. The first reconnection takes place in the lower atmosphere and is due to a slow, but continuous, magnetic flux cancellation near the filament. The second reconnection, which is explosive and takes place in the corona, is caused by the eruption of the filament which triggers a two-ribbon flare. The analysis is based on $H\alpha$ data acquired by THEMIS operating in IPM mode, $H\alpha$ data and magnetograms obtained at the Big Bear Solar Observatory, and 171 Å images taken by TRACE.

Key words. Filaments – Magnetic Reconnection – Flares

1. Introduction

Observations show that filaments form above the polarity inversion line (PIL) and that changes in their configuration are closely related to energetic events like flares and coronal mass ejections (Tandberg-Hanssen (1995)).

Recent models of filament formation require flux convergence and cancellation as basic precursors, and the presence of a dip in the central part of a magnetic arcade, able to support the cool and dense prominence plasma against gravity (Martens and Zwaan (2001), Antiochos and Klimchuk

(1991), Antiochos, Dahlburg and Klimchuk (1994)).

As far as the filament eruption is concerned, flux emergence, twisting and/or shearing and subsequent reconnection are considered all probable causes which could lead to a catastrophic loss of equilibrium of the filament (Heyvaerts, Priest and Rust (1977), Priest and Forbes (2002)).

In this context we describe the activation and eruption of a filament which occurred in the Active Region NOAA 9445 on May 5 2001, and was associated with a two-ribbon flare. We have examined images acquired by the Telescope Heliographique pour l'Etude du Magnetisme et des Instabilites Solaires (THEMIS) along the $H\alpha$ line profile during the pre-flare phase, $H\alpha$ images

Send offprint requests to: L. Contarino

Correspondence to: Dipartimento di Fisica ed Astronomia, Via S.Sofia, 78, Catania, Italy

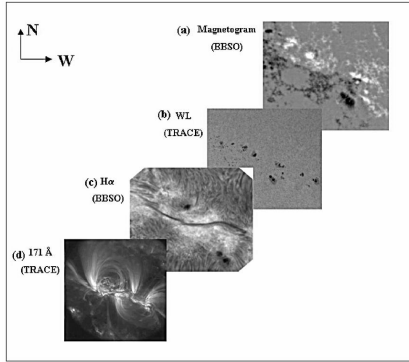


Fig. 1. AR 9445 on May 5, 2001: (a) BBSO magnetogram (fov $\sim 200000 \times 120000 \text{ km}^2$); (b) TRACE WL image (fov $\sim 227500 \times 227500 \text{ km}^2$); (c) $H\alpha$ image taken by BBSO (fov $\sim 120000 \times 120000 \text{ km}^2$); (d) TRACE image at 171 \AA (fov $\sim 358000 \times 358000 \text{ km}^2$).

and longitudinal magnetograms taken at the Big Bear Solar Observatory (BBSO) and coronal images taken by the Transition Region and Coronal Explorer (TRACE) at 171 \AA .

2. Observations and Data Analysis

AR 9445 was seen rising at the east limb on April 29, 2001 (average latitude 25 North) and setting on May 10, 2001. Fig. 1 shows the characteristics of AR 9445 at different atmospheric layers and a BBSO magnetogram, on May 05, 2001.

The data analysis shows an event characterized by the splitting and the eruption of a filament and a successive two-ribbon flare (Contarino et al. (2002), Contarino et al. (2003)).

It is possible to divide the event into two phases:

- filament activation and eruption (16:40 - 17:40 - 18:05 UT).
- two-ribbon flare (18:07 - 18:20 - 19:00 UT)

During the first phase the western end of the filament shows a splitting into two threads (16:40 - 17:40 UT) and then the

northern part rises towards higher levels (17:41 - 18:05 UT). In the second phase a two-ribbon flare of GOES class C6.3 is observed.

We have analysed THEMIS and BBSO sequences of three different sets of chromospheric images: $H\alpha$ center images ($\lambda = 6562.8 \text{ \AA}$), blueshifted images (-0.50 \AA) and red shifted images ($+0.50 \text{ \AA}$).

The images show that about 1.5 hours

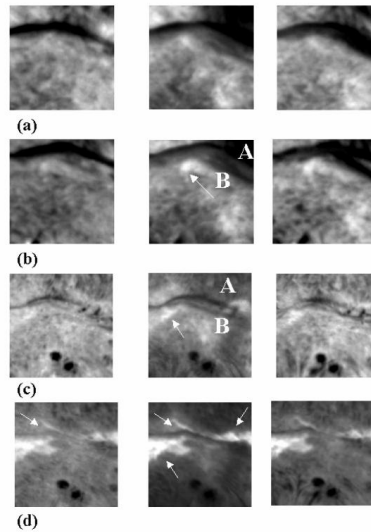


Fig. 2. Sequence of blueshifted (left column), $H\alpha$ center (center column) and redshifted (right column) images acquired by THEMIS at (a) 17:13 and (b) 17:34 U.T (fov $\sim 24500 \times 24500 \text{ km}^2$) and by BBSO at (c) 18:01 and (d) 18:24 U.T. (fov $\sim 40000 \times 40000 \text{ km}^2$), respectively. North is on the top, west on the right.

before the flare, the western part of the filament slowly breaks into two threads (indicated as A, the northern and B, the southern, Fig. 2). Moreover, all the images show a bright patch located where the filament bifurcates (arrow in the center column of Fig. 2 (b-c)). The area of the bright patch is $\sim 4.9 \times 10^7 \text{ km}^2$.

Ten minutes before the flare peak (GOES peak-flare time is 18:20 UT) the northern

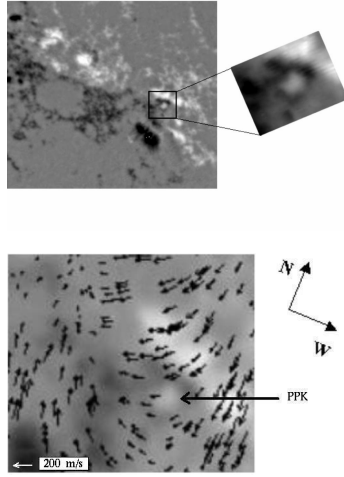


Fig. 3. Upper panel: BBSO magnetogram of AR 9445 obtained on May 5, 2002 at 16:11 U.T (fov $\sim 200000 \times 120000 \text{ km}^2$). White (black) represents positive (negative) polarity. The insert shows an enlarged view of the PPK (fov $\sim 20000 \times 16000 \text{ km}^2$). North is on the top, west on the right. Lower panel: Superposition of the horizontal velocity field on the BBSO high resolution magnetogram taken at 16:00 UT (fov $\sim 11000 \times 11000 \text{ km}^2$).

thread *A* erupts and a $H\alpha$ ribbon appears along the northern boundary of thread *B* (arrows in Fig. 2 (d)).

The upward motion of thread *A* is confirmed by the line of sight velocity maps, obtained by subtracting blueshifted images from redshifted ones. We have determined that the rising velocity of thread *A* is about 10 km/sec.

The analysis of longitudinal high resolution magnetograms, taken at BBSO, shows the presence of a positive polarity knot (PPK) inside a region of negative polarity, which coincides with the site of filament bifurcation and with the bright patch observed in $H\alpha$ images (Fig. 3 (a)). The PPK appears on May 5, at 4:00 UT and after the flare onset, its size and intensity decreases. More precisely,

the PPK area decreases gradually from $2.4 \times 10^7 \text{ km}^2$ to $1 \times 10^7 \text{ km}^2$ during the time interval 16:00 - 19:50 UT.

Moreover, the magnetic flux density in the positive knot decreases from $\sim 250 \text{ G}$, when the filament split, to 120 G at 19:50 UT, while the negative magnetic flux density in the surrounding of the PPK decreases from -160 G to -120 G . Therefore, the PPK may be interpreted as a cancelling magnetic feature (CMF).

We have determined the map of the horizontal velocity field in the photosphere (see Fig. 3 (b)), using the technique of local correlation tracking (November and Simon (1988)). We have found that during the time interval 16:00 - 17:00 UT, the area where the PPK was located, was characterized by a rotational, clockwise motion, with an average velocity of $\sim 120 \pm 18 \text{ m s}^{-1}$. At the same time, the region on the other side of the PIL showed a converging motion toward the PPK.

TRACE images at 171 \AA show that about

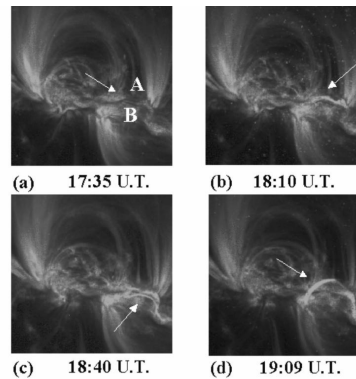


Fig. 4. Sequence of 171 \AA images taken by TRACE between 17:35 and 19:09 U.T., before, during and after the flare (fov $\sim 189000 \times 189000 \text{ km}^2$). North is on the top, west on the right.

2.5 hours before the flare peak, the western part of the EUV filament channel is characterized by the same bifurcated shape of the $H\alpha$ filament. The site where the upper thread *A* of the filament was previously

observed (Fig. 4 (a)) brightens during the pre-flare phase (Fig. 4 (b), probably due to hot plasma rising with the erupting filament). During the main-phase of the flare it is possible to observe an increase in brightness in a loop-like structure which is apparently parallel to the EUV filament channel of thread B (Fig. 4 (c)) and after the appearance of a post-flare loop system (Fig. 4 (d)).

3. Discussion and Conclusions

The observations described in the previous section indicate that the filament eruption occurred in NOAA 9445 is closely related to changes in the magnetic field structure of the surroundings of the filament. This is in agreement with theoretical models presented by Heyvaerts, Priest and Rust (1977). It is therefore plausible that this filament destabilization and eruption might be due to a low-lying reconnection process between an "old" magnetic arcade supporting the filament and a cancelling magnetic feature (CMF). Initially, the field lines supporting the filament had a dip in their central part, while the farthest from the PIL are above the filament and contain it. The field lines of the CMF, located on the southern part of the filament (i. e. on the left of the main PIL), have opposite direction compared to main arcade field lines. The map of the horizontal velocity fields shown in Fig. 3 (b) indicates that both the CMF and the region on the right of the PIL are characterized by motions which might have as a result the close approaching of CMF field lines with low arcade field lines. Therefore a magnetic configuration appropriate for a reconnection process in the low atmosphere may set in. Later, after this low-lying reconnection has taken place, the field line topology has changed and, consequently, the equilibrium conditions may have changed. The filament splits into two

parts and thread *A* erupts. This eruption causes a second reconnection at coronal levels, so that it is possible to observe the appearance of a post-flare loop system.

Therefore, these observations may be interpreted in terms of a two-step process. A first low-lying, slow-mode reconnection occurring at a low temperature ($T \sim 10^4 - 10^5$ K) between the CMF and the arcade supporting the filament, which induces the filament destabilization and its rise toward the corona, and a successive fast reconnection, taking place in higher arcade loops while the filament rises in the corona, occurring at higher temperature ($T \sim 10^6 - 10^7$ K).

Acknowledgements. The authors wish to thank THEMIS staff for their efficient support in the observations, TRACE team for their open data policy and the free diffusion of SolarSoftWare, and BBSO staff for their continuous engagement in observations.

References

- Antiochos, S.K., Klimchuk, J.A., 1991, *ApJ*, 378, 372.
- Antiochos, S.K., Dhalburg, R.B., Klimchuk, J.A., 1994, *ApJ*, 420, L41.
- Contarino, L., Romano, P., Zuccarello, F., Yurchyshyn, V.B., Proc. in *Solar variability - from core to outer frontiers*, 2002, ESA SP 506, 573.
- Contarino, L., Romano, P., Yurchyshyn, V.B., Zuccarello, F., 2003, *Sol.Phys.*, submitted.
- Heyvaerts, J., Priest, E.R., Rust, D.M., 1977, *ApJ*, 216, 123.
- Martens, P.C.H., Zwaan, C., 2001, *ApJ*, 558, 872.
- November, L.J., Simon, G.W., 1988, *ApJ*, 333, 427.
- Priest, E.R., Forbes, T.G., 2002, *Astron. Astrophys. Review*, vol. 10, n.4, 313.
- Tandberg-Hanssen, E., 1995, *The Nature of Solar Prominences*. Kluwer Academic Publishers, Dordrecht.